

Reviewer #1:

The manuscript presents divergence and vorticity data sets from radar wind profilers in the Beijing metropolitan region separated in four triangles spanned by the radar wind profilers mesonet in this region. The authors show the derivation of the vorticity and divergence from the horizontal wind data. They present a comparison to ERA5 and propose the method for short time forecasts of rainfall events.

Data quality:

The data sets are accessible via Zenodo. The data is of good quality and interesting. However, the metadata is not documented very well, especially in the netCDF files. This needs to be improved.

I consider the manuscript suitable for being published in ESSD after the following points have been addressed:

Response: We appreciated tremendously your constructive and thorough comments, which help improve much the quality of our manuscript. We have addressed the reviewer's concerns one by one to the best of our ability. For clarity purpose, here we have listed the reviewers' comments in plain font, followed by our response in bold italics, and the modifications to the manuscript are in italics.

Major comment:

Data sets on Zenodo: Please use the possibility to include metadata (attributes) to the netCDF files. It should be possible to interpret and use them even without the readme file. The global attributes should include at least title, authors, institutions, version, contact, and date, furthermore the definitions of the triangles with the coordinates of the corners. The variable attributes should include the long name of the variable and the units. The short name according to CF standard names (<https://cfconventions.org/Data/cf-standard-names/current/build/cf-standard-name-table.html>) would be nice as well. The definition of the time axis should be clear within the files, i.e. at least the start time and the interval length must be mentioned. The same would be nice for the level coordinate.

Response: Per your suggestions, we have created a new dataset on Zenodo (<https://doi.org/10.5281/zenodo.15297207>) with a detailed metadata, which include all the necessary information and definitions. I hope you are satisfied with these revisions.

Minor comments:

1. Data sets on Zenodo: I would suggest to add two additional coordinates for time and altitude with UTC timestamps and heights above sea level.

Response: Both coordinates and heights have been added in the new Dataset on Zenodo.

2. I noticed that the minimum and maximum values of divergence and vorticity are a factor of 2 larger for triangle 2 compared to the other triangles. Why is this? I suggest to add a paragraph to the manuscript where you analyse the differences between the four triangles and also give some interpretation.

Response: The differences for the range of divergence and vorticity arise from the area of triangle that varies by triangles. As given in the calculation formulas, the divergence and vorticity are highly dependent on the denominator (i.e., the area for a given triangle). To be more specific, the value of divergence and vorticity is inversely proportional to the area of triangle. Therefore, the magnitudes of calculation results are larger for triangle 2, which are attributed to the smallest area of triangle 2.

The above interpretation has been added in Section 2.4.

3. Suggestion: Add a rain flag to the data sets on Zenodo.

Response: Done as suggested.

4. Section 2.1: I am missing more specific information about the RWPs. What type are they, what's their accuracy for the wind measurements, give a brief introduction to the measurement principle.

Response: We have added more specific information about the RWP's measurement principle and its inherent uncertainty for the wind measurements in Section 2.1 in this revision, which is shown as follows:

“These RWPs deployed in Beijing are Ce Feng Leida-6 (CFL-6) Tropospheric Wind Profilers, which are produced by the 23rd Institute of China Aerospace Science and Industry Corporation (Table 1).

Table 1. General characteristics of the CFL-6 radar wind profiler

Parameters	Values
Direction accuracy	$\leq 10^\circ$
Speed accuracy	1.5 m s^{-1}
Vertical resolution	120 or 240 m
Minimum height	150 m
Maximum height	10110 m
Averaging time	6-60 min
Operating frequency	1360 MHz
Gain	33 dB
Peak power	9.6 kW
Pulse width	0.8 or 1.6 μs

The RWPs detect vertically resolved wind fields by transmitting and receiving electromagnetic beams in five directions, including a zenith and four inclined directions of 15° in the east, south, west and north, respectively. By analyzing the Doppler shifts of radial velocities from any three beams, horizontal and vertical wind components are resolved. However, the falling of small targets (particulate scatterers) and raindrops may cause the error of vertical velocity in such a way that vertical velocity cannot usually be used directly (Angevine, 1996; Wang et al., 2014; McCaffrey et al., 2017). The fluctuating component of the horizontal velocity is not affected by these errors since it is much larger in magnitude.”

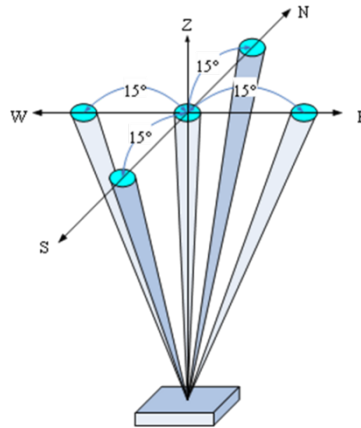


Figure R1. Schematic diagram of wind profile radar beam. (This figure was found online to introduce the measurement principle to you, so it isn't put in this article)

5. Section 2.2, l. 137 ff.: This is just a suggestion. If I got this correctly, $i = 1, 2, 3$ counts the triangle corners which are called A, B, C. So essentially, the index 1, 2, 3 is the same as A, B, C, respectively. You could get rid of this „double naming“ by saying $i = A, B, C$ which would clarify that it means the same thing and adapt the following equations accordingly.

Response: *Amended as suggested.*

6. Section 3: I found the comparison between the RWP data and ERA5 not very convincing, especially since the correlations shown in figure 3 are so small that it is hard to conclude that they are correlated at all. Is there any other data set you can use to verify your data?

Response: *To ensure the data quality of the RWPs, the horizontal wind dataset is validated against radiosonde measurements. The results show that the horizontal winds derived from RWPs in the heights of 0.51–4.11km AGL are believed to be reliable enough with the correlation exceeding 0.8. This gives us confidence to believe in the high quality of our divergence and vorticity dataset. The uncertainties of RWP measurements are given in our response to your comment # 10.*

On top of this, we further compare the dynamic variables from RWP measurements against NCEP reanalysis. It is well known that the ERA5 and

National Center for Environment Prediction (NCEP) are most promising and commonly used reanalysis data sources in terms of characterizing the evolution of atmospheric environment. In contrast to ERA5(0.25°×0.25° at hourly intervals), NCEP reanalysis has lower spatial and temporal resolution(2.5°×2.5° at 6-hourly intervals). It relies more on interpolation during the process of data assimilation, so it underestimates the horizontal wind speeds and dynamic parameters even more. As shown in Figure R2 and R3, the results are basically similar to the comparison between the RWP data and ERA5 except for the much smaller value range distribution. The correlations between the RWP and NCEP shown in Figure R3 are smaller than those between the RWP and ERA5 shown in figure 3, especially at the higher altitudes. Thus, the results above are consistent with the conclusions and prove the accuracy of retrieved wind fields and the differences between observation with higher resolution and reanalysis data by interpolation.

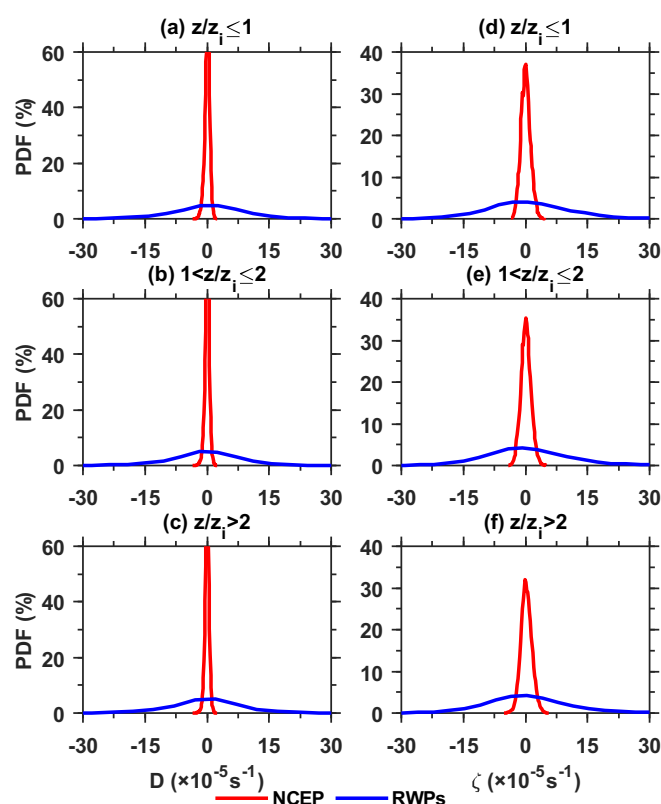


Figure R2. The probability density function (PDF) of horizontal divergence (D) estimated from the measurements of RWPs mesonet (blue line) and NCEP

reanalysis (red line) at the height of (a) $z/z_i \leq 1$, (b) $1 < z/z_i \leq 2$, and (c) $z/z_i > 2$; (d) –(f) the same as (a)–(c) but for the PDF of vertical vorticity (ζ).

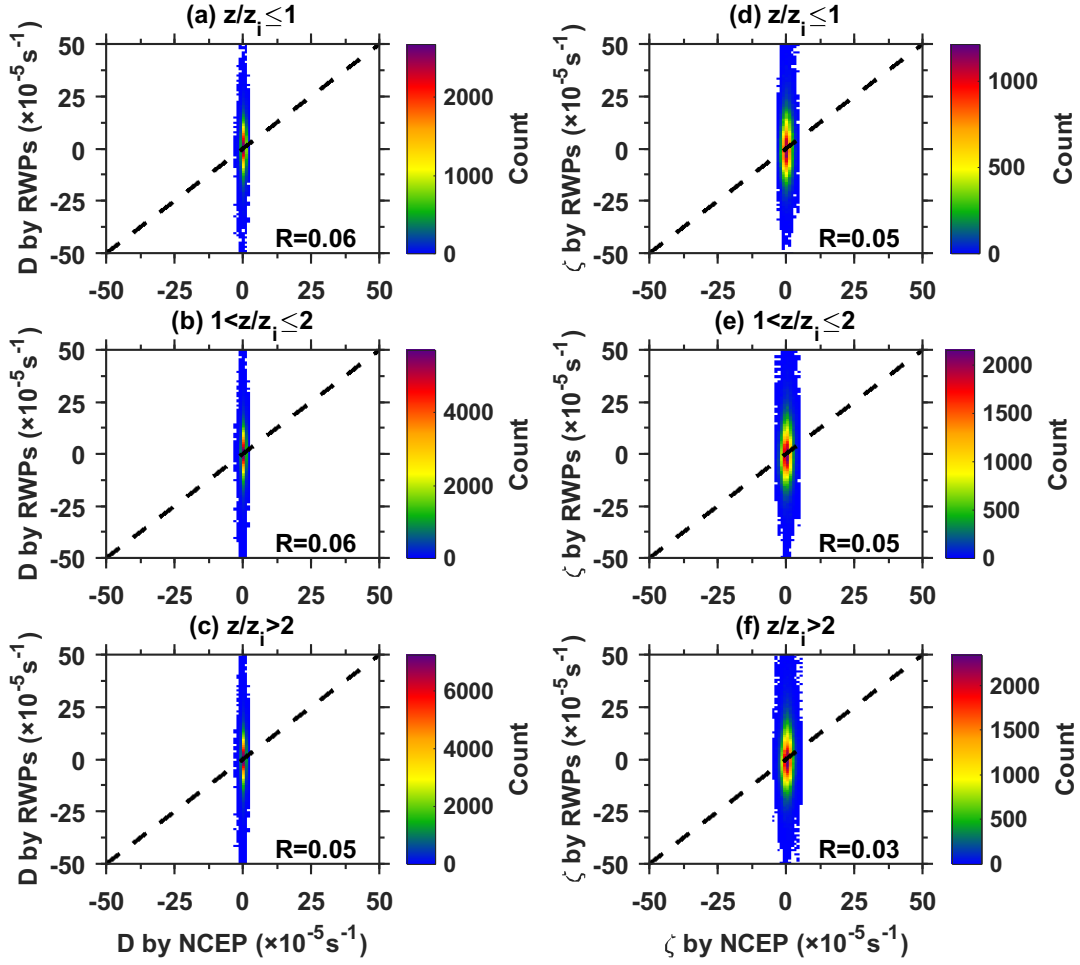


Figure R3. Scatterplots of the horizontal divergence (D) from the measurements of RWPs mesonet versus NCEP reanalysis at the heights of (a) $z/z_i \leq 1$, (b) $1 < z/z_i \leq 2$, and (c) $z/z_i > 2$ with the 1:1 line shown as black-dashed lines, respectively. The color bar indicates the counts of data points. (d)–(f) the same as (a)–(c) but for the vertical vorticity (ζ).

7. Please add references to l. 190.

Response: The following references have been added.

References:

Adler, B. and Kalthoff, N.: Multi-scale transport processes observed in the boundary layer over a mountainous island, *Bound.-Lay. Meteorol.*, 153, 515–537,

<https://doi.org/10.1007/s10546-014-9957-8>, 2014.

Dai, C., Wang, Q., Kalogiros, J. A., Lenschow, D. H., Gao, Z., and Zhou, M.: Determining boundary-layer height from aircraft measurements, *Bound.-Lay. Meteorol.*, 152, 277–302, <https://doi.org/10.1007/s10546-014-9929-z>, 2014.

Dodson, D. S. and Small Griswold, J. D.: Turbulent and boundary layer characteristics during VOCALS-REx, *Atmos. Chem. Phys.*, 21, 1937–1961, <https://doi.org/10.5194/acp-21-1937-2021>, 2021.

Su, T. N., Li, Z. Q., and Zheng, Y. T.: Cloud-Surface Coupling Alters the Morning Transition from Stable to Unstable Boundary Layer, *Geophys. Res. Lett.*, 50, e2022GL102256, <https://doi.org/10.1029/2022gl102256>, 2023.

8. I did not get the definition of z_i . Is it the PBL height or something else. Please rephrase the definition in l. 193.

Response: *There are significant differences between the wind field in the PBL and the upper atmosphere, an important parameter z_i is defined to better reveal the characteristics of divergence and vorticity at different heights. The definition of z_i has been rephrased as followed:*

“Considering that the altitude z is used in this study instead of height above ground level, z_i for a given triangle equals to the terrain height plus and PBL height. To better reveal how the divergence and vorticity vary with PBL, z can be normalized by z_i to provide a nondimensional vertical coordinate for horizontal divergence and vertical vorticity in the following analyses. The layers at the range of 0.51–4.11 km AMSL is classified as near-surface, low-level, and mid-level layer according to the criterion of $z/z_i \leq 1$, $1 < z/z_i \leq 2$, $z/z_i > 2$, respectively”

9. Please also rephrase the following lines 195-197. As far as I understand, you are not setting z/z_i to 2 or 1 but looking at these specific altitudes, right? In the current formulation it sounds as if z/z_i is a parameter which can be freely chosen, but it is a coordinate.

Response: We are sorry to make you confused. Actually, we want to separate different altitude layers to near-surface, low-level, and mid-level layer according to z_i . For exmaple, when $z_i=1$ km, the layers below 1 km, from 1 to 2 km, above 2km AMSL is seen as near-surface layer, low-level, and mid-level layer, respectively. The related expression has been rephrased.

10. You discuss in section 3 why ERA5 is less reliable than the RWP observations and why the pdfs are steeper. However, there are probably also some uncertainties in the RWP measurements and approximations needed. Please comment on this.

Response: We have added some necessary analyses about the RWP measurements and validated the winds from RWPs against those from radiosonde in Sections 2.1.and 2.2, which are shown as follows:

“To ensure the integrity of the data, a test for the acquisition rate of the horizontal wind profiles spanning a whole year of 2023 is conducted. As shown in Figure 1b, the observations below 4.11 km AGL for six RWPs relatively meet the requirements of continuity in time with the average missing rate less than 20%. Therefore, the horizontal winds derived from six RWPs at the heights of 0.15–4.11 km AGL in 2023 are collected in this study.”

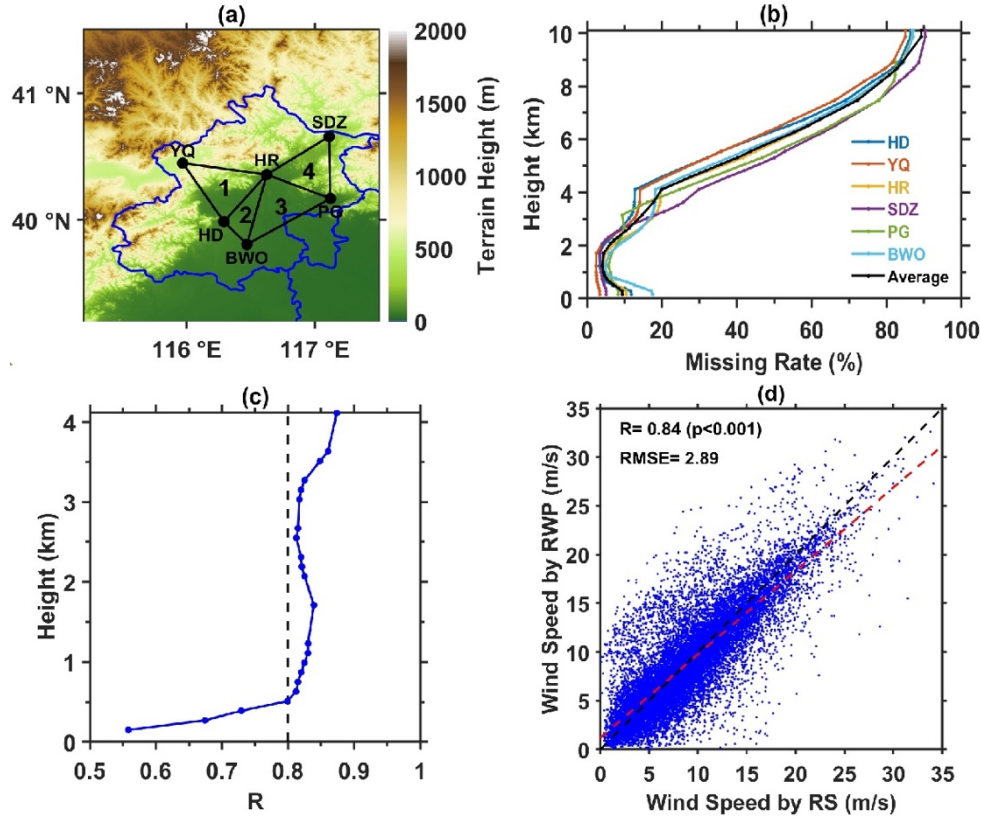


Figure 1. (a) Locations of the six radar wind profiler (RWP) stations (black dots). The blue line denotes the administrative boundaries at the provincial level. Four black triangles with number denote the regions used to calculate the horizontal divergence and vertical vorticity with the triangle method. (b) The missing rate of horizontal wind speeds at different heights derived from six RWPs. (c) Vertical profile of the correlation coefficient (R) between horizontal wind speeds derived from the RWP and those from the upper-air soundings (RS) at the Beijing Weather Observatory (BWO). (d) Scatterplots of the horizontal wind speeds at the range of 0.51–4.11 km above ground level (AGL) from the RWP versus RS at the BWO. The red and black dashed lines denote the linear regression and 1:1 line respectively.

Besides, we rephrased the revised Section 2.2 entitled with **Evaluation of horizontal winds of RWP**, which is shown as follows:

To further evaluate the data quality of the RWPs, horizontal wind speeds at every level from the BWO are validated against the coincident radiosonde measurements. Upper-air sounding balloons are launched at the BWO twice daily at

0800, and 2000 Local Standard Time (LST), providing the vertical profiles of temperature, pressure, relative humidity, and horizontal winds with a vertical resolution of 5–8 m (Guo et al., 2021b). During summer months (June-July-August), an intensive observation campaign has been conducted at most radiosonde stations of China with an additional balloon launches at 1400 LST. As shown in Figure 1c, the correlation coefficient (R) is found greater than 0.8 from 0.51 to 4.11 km AGL. Nevertheless, the accuracy and reliability of the RWP data below 0.51 km is limited by the interference of near-surface clutter. Scatterplots obtained by aggregating all the samples between 0.51 and 4.11 km AGL produce a correlation coefficient (R) value as high as 0.84 (Figure 1d). Thus, the horizontal winds derived from RWPs in the heights of 0.51–4.11km AGL are believed to be reliable enough and then be adopted here for the generation of atmospheric dynamic dataset.

11. 1. 228: The method of the precipitation measurements should be mentioned.

Response: *Per your kind suggestions, the methods have been supplemented in Section 2.3, which is shown as follows:*

“Rainfall at 1-min interval is directly acquired from the rain gauge measurements at automated surface stations over Beijing. Here, 6-min accumulated rainfall is synchronized with the RWP measurements at 6-min interval. These rain gauge measurements have undergone rigorous quality control and are publicly available by the China Meteorological Administration.”

The introduction of triangle-area-averaged rainfall is added in Section 5.1, which is shown as follows:

There are 29, 42, 49, and 15 rain gauges in triangles 1, 2, 3, and 4 respectively. For each triangle, The triangle-area-averaged rainfall amount is obtained from the average of 6-min accumulated rainfall from all rain gauges in that triangle.”

12. Fig. 4: For comparison it would be good to show the same plots for times without rain events. Otherwise it is hard to interpret how the shown behaviour is specific for rain events. This should be also further discussed in section 4.1. 240 ff.

Response: Per your suggestion, we added the same plots for times without rain events in Figure 4a and b, then compared the temporal patterns between non-precipitation and precipitation environments as followed:

“Figure 4a and 4b present the normalized contoured frequency by altitude (NCFAD) for all profiles of the horizontal divergence and vertical vorticity as observed by the RWP mesonet in non-precipitation days, respectively. Specifically, the values of horizontal divergence and vertical vorticity are overall distributed around zero above 2.5 km AMSL. The magnitude of vorticity is greater than that of divergence with more vertical fluctuation in the mid-troposphere. Weak diffluence as indicated by positive divergence values exists in the lower troposphere below 2 km AMSL. By comparison, the pre-storm dynamic environment within 1-hour preceding rainfall events (Figure 4c and 4d) exhibits significant difference, which implies the presence of complex vertical motion in this unstable atmosphere. The divergence below 1 km AMSL significantly concentrates from $-5 \times 10^{-5} \text{ s}^{-1}$ to zero before rainfall events (Figure 4c). As indicated in Figure 4d, the lowest layer is dominated by positive vorticity centering near 1 km AMSL.

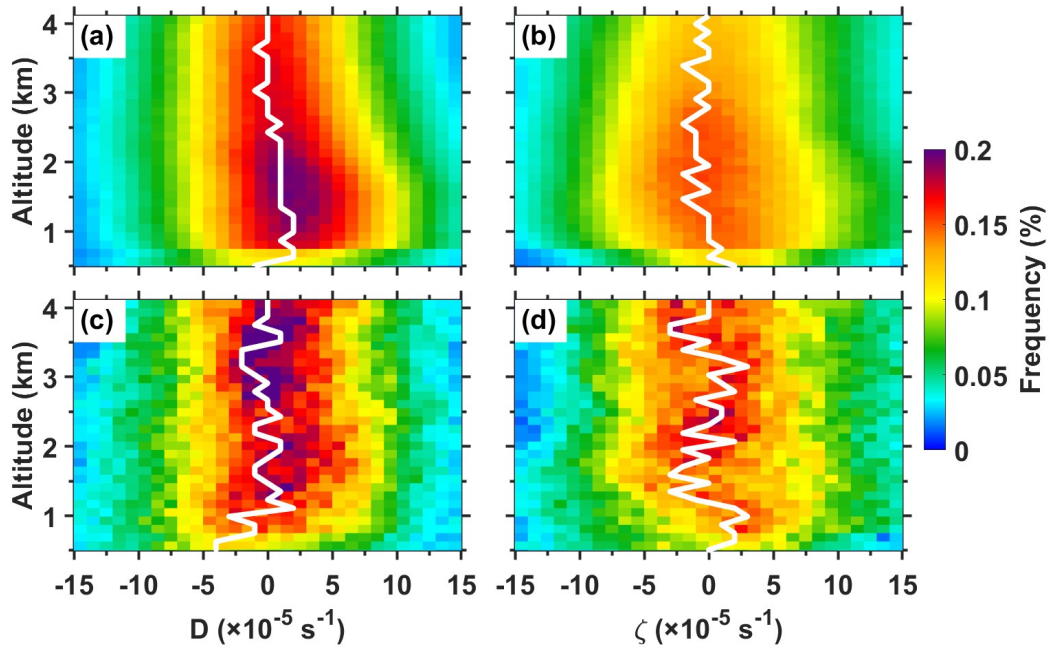


Figure 4. Normalized contoured frequency by altitude (NCFAD) for the horizontal divergence (a) and vertical vorticity (b) between 0.51-4.11 km AMSL as calculated by the RWP mesonet measurements in non-precipitation days of 2023 in Beijing. The white line represents the profile of maximum frequency distribution. (c) and (d) Same as (a) and (b), except for the frequency distribution within 1-hour preceding rainfall events.

By using dynamic parameters with higher temporal resolution obtained from the RWPs mesonet, our aim is to further explore potential patterns or trends in the pre-rainfall convection environment during the lead time. Figures 5a and 5b show the evolutions of average profiles of horizontal divergence and vertical vorticity at 12-min interval before the occurrence of rainfall events. The significant increase in average convergence below 1.5 km AMSL within 48 min ahead of precipitation (Figure 5a) is largely contributed to the fact that near-surface air tends to strongly converge into the pre-squall mesotrough when convective system approaches. The main convection was collocated with low-level convergence and midlevel divergence placed ahead of the precipitation center. These patterns are consistent with previous studies (Wilson and Schreiber, 1986; Zhang et al., 1989; Qin and Chen, 2017; Yin et al., 2020).

Similarly, the increase in vertical vorticity shown in Figure 5b might be associated with significant horizontal wind shear. The preexisting ambient wind field before the arrival of MCS is critical to system organization since the orientation of its vertical shear directly influences an asymmetric precipitation structure with mesoscale rotation. In addition, the mesoscale convective vortex (MCV) may be resulted from deep and moist convection prior to the passage of the MCS (Wang et al. 1993). Trier et al. (1997) indicated that the MCS-induced horizontal flow and its associated vertical shear are critical factors which influence the development of the vortex. This southwesterly flow, enhanced by the MCV circulation, transports moisture northward in the lower troposphere, thereby creating potential instability ahead of the vortex center. Such an environment is favorable for convection and further lead heavy precipitation (Johnson et al., 1989; Hendricks et al., 2004; Lai et al., 2011).”

13. Section 4 and 5: You mention that the RWP mesonet can be used for rain forecasting. I am missing a more detailed explanation on how this works. Please add more discussion.

Response: Per your kind suggestions, we added more detailed explanation about the potential application of the RWP-derived divergence profiles for capture the CI and subsequent rainfall in section 4.2 by a case study.

“Due to the direct connection between horizontal divergence and vertical motion, we attempt to further discuss how the RWP-derived divergence could practically benefit short-term forecasting of a convective rainfall event. The evolution of 30-min accumulated rainfall from rain gauge measurements is given in Figure 6. After 0400 LST 22 July, 2023, an early-morning event occurred in Beijing with a maximum rainfall rate exceeding 10 mm within 30 minutes. This event was associated with the transport of moisture as the subtropical moved northward. The main region of precipitation was located to the southeast of Beijing before 0500 LST, there was no significant rainfall within the RWP mesonet (Figure 6a, b). As the major convective storm slowly propagated northward and approached the edge of triangle 3 after 0500

LST (Figure 6c), the precipitation then took place. Interestingly, a few new cells at the meso- γ -scale formed in triangle 1 at the same time (Figure 6d-e) and expanded rapidly to other triangles (Figure 6f-h). The uneven precipitation caused by these isolated and scattered convection cells was a difficult problem in monitoring and nowcasting. Of relevance to this study was the potential application of the RWP-derived divergence profiles for capture the CI and subsequent rainfall.

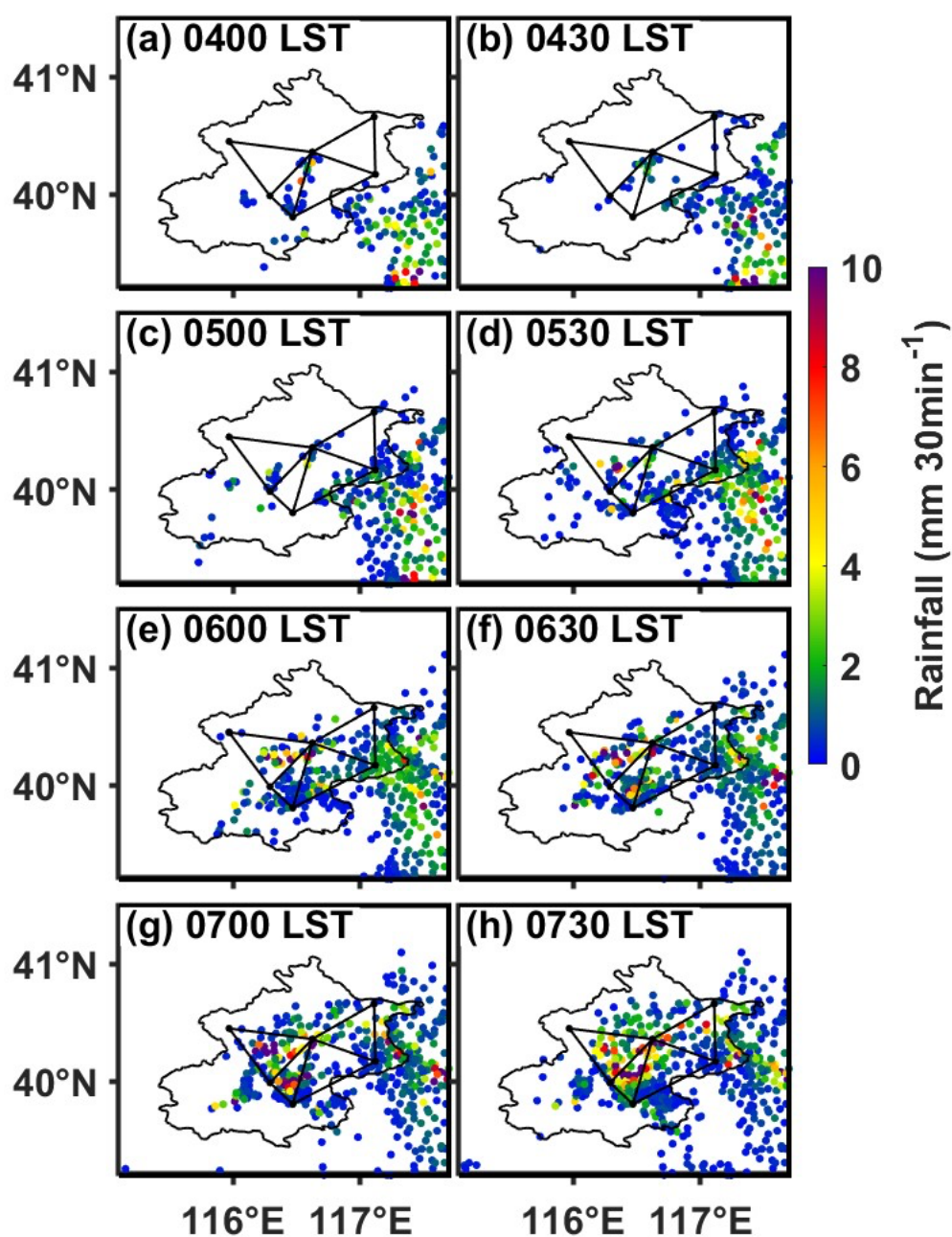


Figure 6. Accumulated precipitation (mm 30min⁻¹; colored dots) at (a) 0400 (b) 0430, (c) 0500, (d) 0530, (e) 0600, (f) 0630, (g) 0700 and (h) 0730 LST 22 July, 2023. The RWP mesonet is also plotted (see Figure 1a for the location).

Figure 7a–d display the time series of the rainfall rates and vertical profiles of the area-averaged divergence during the period of 0400–0730 LST 22 July, 2023 in triangles 1–4 respectively. Specifically, one can see the presence of weak convergence below 2 km AMSL with significant divergence above after 0400 LST in triangle 1 from Figure 7a. Subsequently, the convergence layer deepened up to 3.5 km AGL from 0430 LST. The low-level convergence simultaneously strengthened with the maximum value of $-1.4 \times 10^{-4} \text{ s}^{-1}$ near 1 km AMSL at 0448 LST. The signals of prevailing convergence in the lower troposphere provided favorable upward motions for the important lifting of water vapor in the PBL in advance of the convective rainfall. The more intense convergence and upward motion were also well detected in triangle 2 below 1.23 km AMSL after 0448 LST (Figure 7b) which coincided with the generation of rainfall in triangle 1. The inflow over triangle 2 could be attributed to the fact that cold downdraft air in triangle 1 tended to converge into the mesotrough ahead of convection. Even considering the strongest convergence of triangle 2 was resulted from the smallest area to a certain extent, such a significant enhanced trend was evident. Similarly, the rainfall in triangle 2 started at 0530 LST closely related to pronounced convergence and upward motion in the lower troposphere.

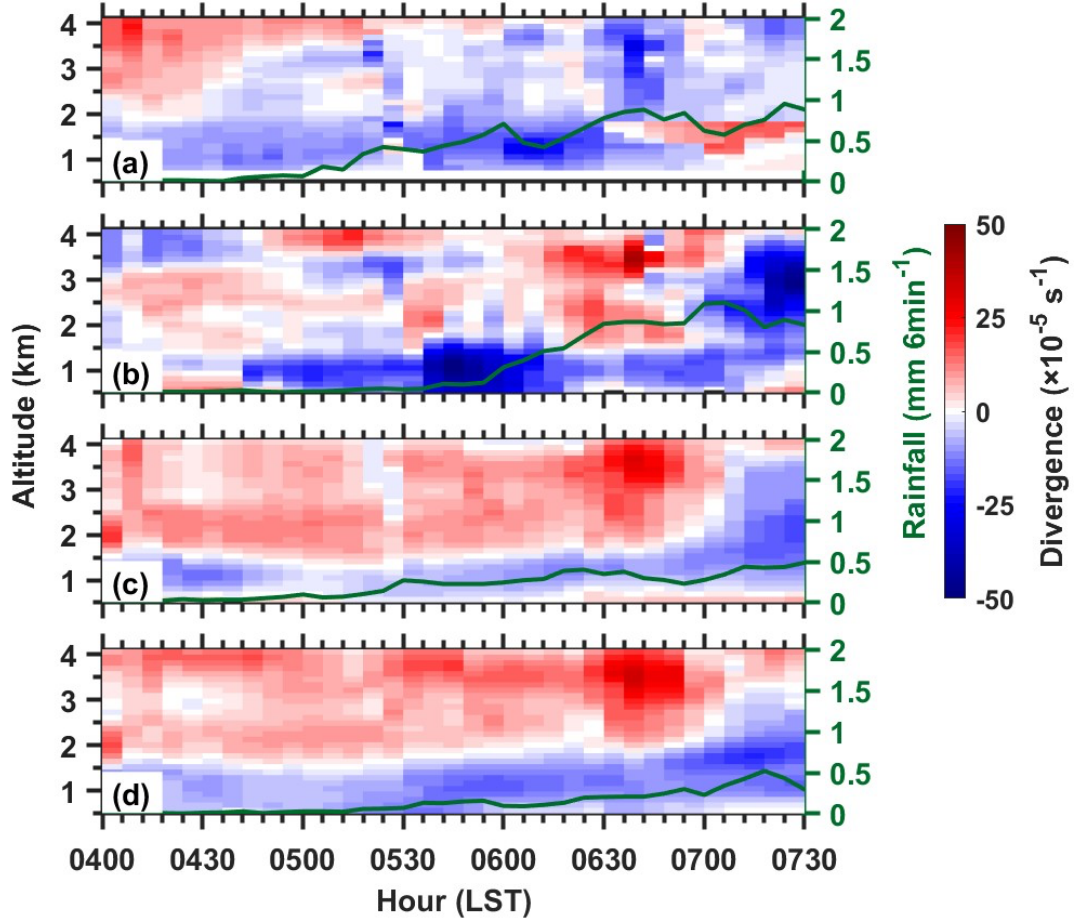


Figure 7. The vertical profiles of the triangle-averaged divergence (10^{-5} s^{-1} , shading) derived from the RWP mesonet in Beijing at 120 m vertical resolution between 0.51 and 4.11 km AMSL at 6-min intervals during the period of 0400–0730 LST 22 July, 2023 for (a) triangle 1, (b) triangle 2, (c) triangle 3, and (d) triangle 4 (see their distributions in Figure 1a). Green-dotted lines represent the triangle-area-averaged rainfall amount ($\text{mm } 6\text{min}^{-1}$).

As shown in Figure 7c and 7d, the relationship between vertical profiles of divergence and rainfall for triangle 3 and 4 during the rainy period was analogous to that for triangle 1 and 2. Nevertheless, triangle 3 and 4 experienced relatively weaker low-level convergence below 1.5 km AMSL. The presence of dominated divergence layer above is not conducive to the extension of upward movement and formation of convective clouds. The weaker peak area-averaged rainfall rate was seen in triangle 3 and 4 in contrast. Clearly, it has been proved that the RWP mesonet has the capability of detecting the continuous vertical profiles of divergence leading to the

onset of precipitation at high spatial and temporal resolutions. However, the development of convection is also affected by many other thermal and dynamic variables, it should be noted that it's feasible to qualitatively determine the change of rainfall rather than quantitatively."

14. I do not understand l. 250 f. Please rephrase this sentence.

Response: The sentence has been rephrased as:

"Specifically, the values of horizontal divergence are distributed around zero above 1 km AMSL (Figure 4a)."

15. l. 258: Please introduce the abbreviation CI.

Response: "CI" refers to the abbreviation of "convection initiation".

16. l. 287 ff.: Are the data of the wind fields also published somewhere? If yes, please cite.

Response: The data of the wind fields hasn't been published.

Technical comments:

1. Please check the use of singular and plural of nouns, e.g. l. 66 stations, l. 111 "datasets" or "is" and „has“, l. 163 positions.

Response: Corrected.

2. Please also check if there are articles before nouns when necessary, e.g. l. 197 the two dynamic parameters (or specify the parameters), l. 511 the grey layer , l. 317 the surface.

Response: Amended as suggested.

3. l. 83: typo in calculate

Response: Corrected.

4. l. 278: typo twice "by the"

Response: Corrected.

5. L. 301: typo "which" is too much

Response: "which" has been deleted.

6. Equations in section 2.2: The primes (A' etc.) are not visible. Please improve their visibility.

Response: Amended as suggested.

7. Punctuation characters are missing for all equations.

Response: Punctuation characters have been added.

8. The ESSD guidelines suggest to use a sans-serif font for the figures.

Response: Amended as suggested.

Reviewer #2:

This manuscript presents a high-resolution dataset of horizontal divergence and vertical vorticity profiles derived from a radar wind profiler mesonet in Beijing. Utilizing the triangle method on continuous wind measurements throughout 2023, the study provides important datasets into mesoscale convective processes and the precursors to convective rainfall events. The authors demonstrate that these radar-derived parameters differ from ERA5 reanalysis, highlighting potential shortcomings of the latter at capturing mesoscale systems. In general, the scientific merits of the dataset are clear. I would recommend the publication of this paper after minor revisions.

Response: Thank you for your positive evaluation. We appreciated tremendously your constructive and thorough comments, which help improve much the quality of our manuscript. We have addressed the reviewer's concerns one by one to the best of our ability. For clarity purpose, here we have listed the reviewers' comments in plain font, followed by our response in bold italics, and the modifications to the manuscript are in italics.

Minor comments:

1. The manuscript would benefit from a clearer discussion regarding the uncertainties inherent in RWP measurements. It is recommended to acknowledge potential biases caused by vertical velocity retrieval errors, radar signal attenuation under varying meteorological conditions, and sampling inaccuracies associated with spatial-temporal resolutions.

Response: Per your kind suggestion, we have added more specific information about the RWP's measurement principle and its inherent uncertainty for the wind measurements in Sections 2.1 and 2.2, which are presented as follows:

“The RWPs detect vertically resolved wind fields by transmitting and receiving electromagnetic beams in five directions, including a zenith and four inclined directions of 15° in the east, south, west and north, respectively. By analyzing the

Doppler shifts of radial velocities from any three beams, horizontal and vertical wind components are retrieved. However, the falling of small targets (particulate scatterers) and raindrops may cause the potential biases of vertical velocity in such a way that vertical velocity cannot usually be used directly (Angevine, 1996; Wang et al., 2014). The fluctuating component of the horizontal velocity is not affected under varying meteorological conditions since it is much larger in magnitude.

To ensure the integrity of the data, a test for the acquisition rate of the horizontal wind profiles spanning a whole year of 2023 is conducted. As shown in Figure 1b, the observations below 4.11 km AGL for six RWPs relatively meet the requirements of continuity in time with the average missing rate less than 20%. These relatively low acquisition of the RWP data at high altitude could be attributed to the well-known limitations that the radar signal attenuation constitutes the inherent uncertainty sources. Therefore, the horizontal winds derived from six RWPs at the heights of 0.15–4.11 km AGL in 2023 are collected in this study.

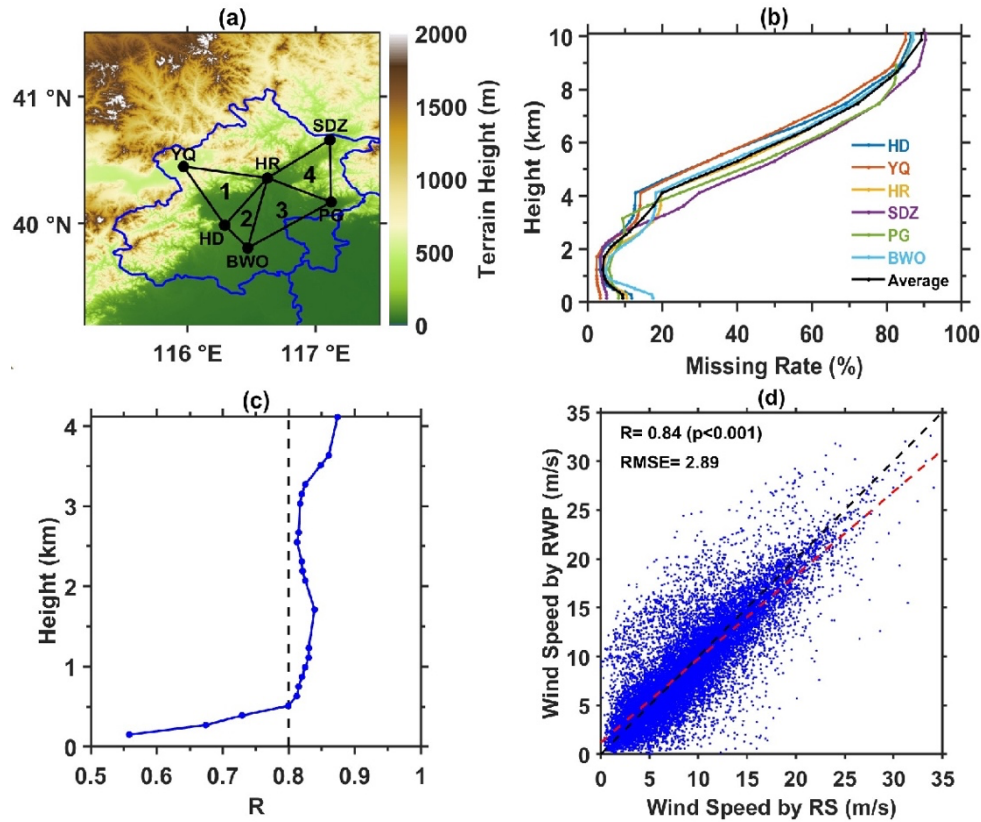


Figure 1. (a) Locations of the six radar wind profiler (RWP) stations (black dots). The blue line denotes the administrative boundaries at the provincial level. Four black triangles with number denote the regions used to calculate the horizontal divergence and vertical vorticity with the triangle method. (b) The missing rate of horizontal wind speeds at different heights derived from six RWPs. (c) Vertical profile of the correlation coefficient (R) between horizontal wind speeds derived from the RWP and those from the upper-air soundings (RS) at the Beijing Weather Observatory (BWO). (d) Scatterplots of the horizontal wind speeds at the range of 0.51–4.11 km above ground level (AGL) from the RWP versus RS at the BWO. The red and black dashed lines denote the linear regression and 1:1 line respectively.

To further evaluate the data quality of the RWPs, horizontal wind speeds at every level from the BWO are validated against radiosonde measurements. Upper-air sounding balloons are launched at the BWO twice daily at 0800, and 2000 Local Standard Time (LST), providing the vertical profiles of temperature, pressure, relative humidity, and horizontal winds with a vertical resolution of 5–8 m (Guo et al., 2020). During summer months (June–August), an intensive observation is added at 1400 LST. From Figure 1c, the correlation coefficient (R) was greater than 0.8 from 0.51 to 4.11 km AGL. Nevertheless, the accuracy and reliability of the RWP data below 0.51 km is limited by the interference of near-surface clutter. Scatterplots obtained by aggregating all the samples between 0.51 and 4.11 km AGL produce a correlation coefficient (R) value as high as 0.84 (Figure 1d). Thus, the horizontal winds derived from RWPs in the heights of 0.51–4.11 km AGL are believed to be reliable enough and then be adopted here for the generation of atmospheric dynamic dataset. ”

2. The representativeness of divergence and vorticity profiles calculated using the triangle method strongly depends on the geometry and spacing of the profiler network. It may be helpful to discuss the potential effects of the heterogeneous urban landscape and complex terrain of the Beijing region.

Response: Per your suggestions, inevitable sampling inaccuracies associated with spatial resolutions have been acknowledged in Section 2.4.

“Specifically, the value of divergence and vorticity is inversely proportional to the area of triangle using the triangle method. Therefore, the magnitudes of results are larger for triangle 2, which could be attributed partly to the smallest area of triangle 2 used for area-averaged calculations compared to those of other triangles. This coincides with the fact that the gradient of velocity between two points, including

$\frac{\partial u}{\partial x}$, $\frac{\partial v}{\partial x}$, $\frac{\partial u}{\partial y}$ and $\frac{\partial v}{\partial y}$, will increase when the distance is shortened.”

Additionally, the accuracy and reliability of the RWP data below 0.51 km is limited by the interference of near-surface clutter. Considering the six RWPs located at different terrain elevations, the horizontal velocities measured by each RWP are interpolated to the same altitude that starts upwards from 0.51 km above mean sea level (AMSL). Therefore, the potential effects of the heterogeneous urban landscape and complex terrain of the Beijing region cannot be discussed temporarily. We consider using wind lidar to compensate for the lack of near-surface observations in the future, which will be beneficial for exploring the bifurcation of flow by the high risings over the built-up area and revealing the meso-scale circulation by the urban heat island effect.

3. Does the triangle method inherently assume linear variations of wind fields across measurement sites? If so, could nonlinear mesoscale dynamics during rapidly evolving convective conditions significantly impact the accuracy or sensitivity of divergence and vorticity retrievals?

Response: The triangle method without the linear interpolation doesn't assume linear variations of wind fields across measurement sites.

4. The authors highlight the potential application of this dataset for rainfall nowcasting. It may be helpful to further discuss how the derived divergence and vorticity profiles could practically benefit short-term forecasting of convective rainfall events

compared to existing methods. Providing clearer context or practical examples could strengthen the manuscript's discussion of its predictive capability and lead-time advantages.

Response: Per your kind suggestions, we added more detailed explanation about the potential application of the RWP-derived divergence profiles for capture the CI and subsequent rainfall in section 4.2 by a case study.

“Due to the direct connection between horizontal divergence and vertical motion, we attempt to further discuss how the RWP-derived divergence could practically benefit short-term forecasting of a convective rainfall event. The evolution of 30-min accumulated rainfall from rain gauge measurements is given in Figure 6. After 0400 LST 22 July, 2023, an early-morning event occurred in Beijing with a maximum rainfall rate exceeding 10 mm within 30 minutes. This event was associated with the transport of moisture as the subtropical moved northward. The main region of precipitation was located to the southeast of Beijing before 0500 LST, there was no significant rainfall within the RWP mesonet (Figure 6a, b). As the major convective storm slowly propagated northward and approached the edge of triangle 3 after 0500 LST (Figure 6c), the precipitation then took place. Interestingly, a few new cells at the meso- γ -scale formed in triangle 1 at the same time (Figure 6d-e) and expanded rapidly to other triangles (Figure 6f-h). The uneven precipitation caused by these isolated and scattered convection cells was a difficult problem in monitoring and nowcasting. Of relevance to this study was the potential application of the RWP-derived divergence profiles for capture the CI and subsequent rainfall.

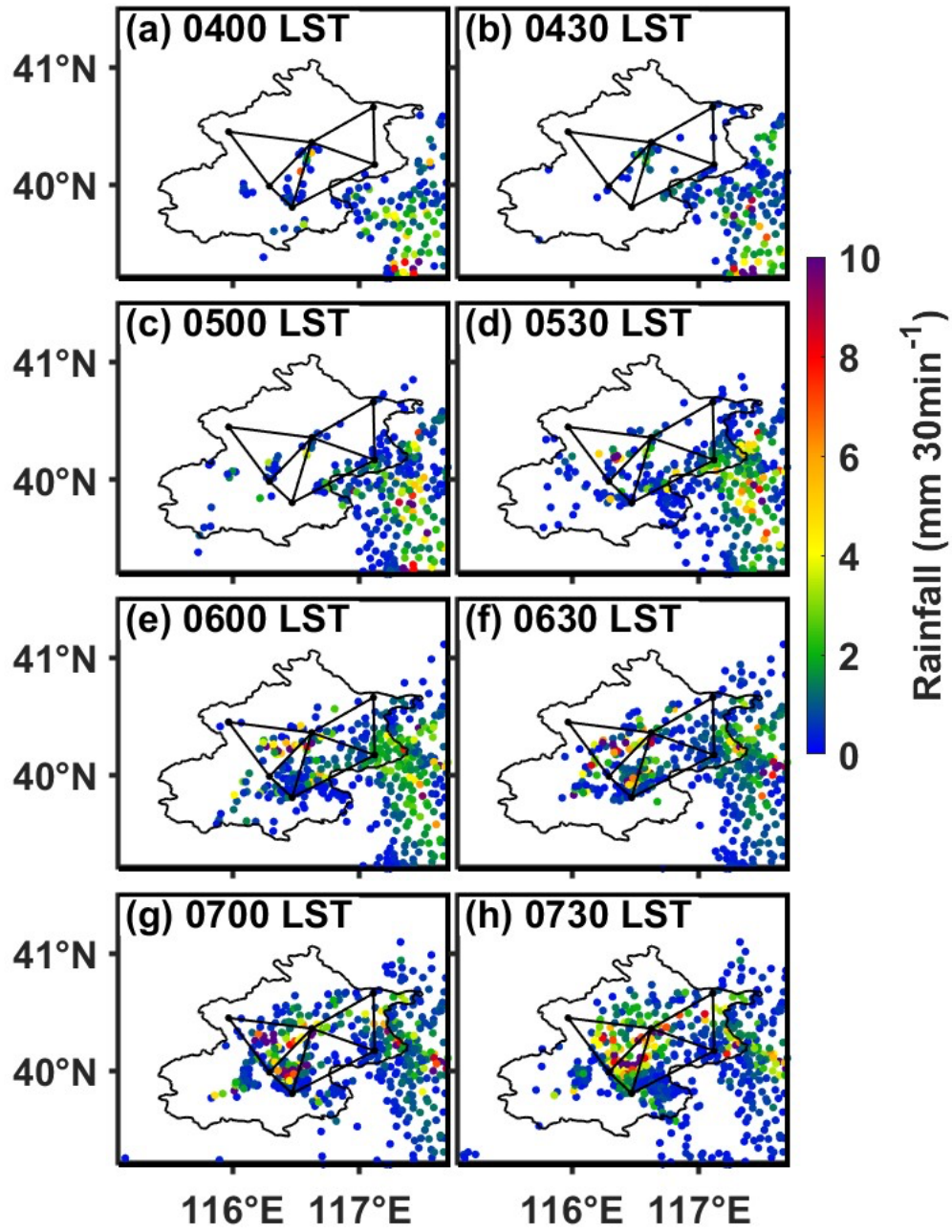


Figure 6. Accumulated precipitation ($\text{mm } 30\text{min}^{-1}$; colored dots) at (a) 0400 (b) 0430, (c) 0500, (d) 0530, (e) 0600, (f) 0630, (g) 0700 and (h) 0730 LST 22 July, 2023. The RWP mesonet is also plotted (see Figure 1a for the location).

Figure 7a–d display the time series of the rainfall rates and vertical profiles of the area-averaged divergence during the period of 0400–0730 LST 22 July, 2023 in triangles 1–4 respectively. Specifically, one can see the presence of weak convergence below 2 km AMSL with significant divergence above after 0400 LST in triangle 1 from

Figure 7a. Subsequently, the convergence layer deepened up to 3.5 km AGL from 0430 LST. The low-level convergence simultaneously strengthened with the maximum value of $-1.4 \times 10^{-4} \text{ s}^{-1}$ near 1 km AMSL at 0448 LST. The signals of prevailing convergence in the lower troposphere provided favorable upward motions for the important lifting of water vapor in the PBL in advance of the convective rainfall. The more intense convergence and upward motion were also well detected in triangle 2 below 1.23 km AMSL after 0448 LST (Figure 7b) which coincided with the generation of rainfall in triangle 1. The inflow over triangle 2 could be attributed to the fact that cold downdraft air in triangle 1 tended to converge into the mesotrough ahead of convection. Even considering the strongest convergence of triangle 2 was resulted from the smallest area to a certain extent, such a significant enhanced trend was evident. Similarly, the rainfall in triangle 2 started at 0530 LST closely related to pronounced convergence and upward motion in the lower troposphere.

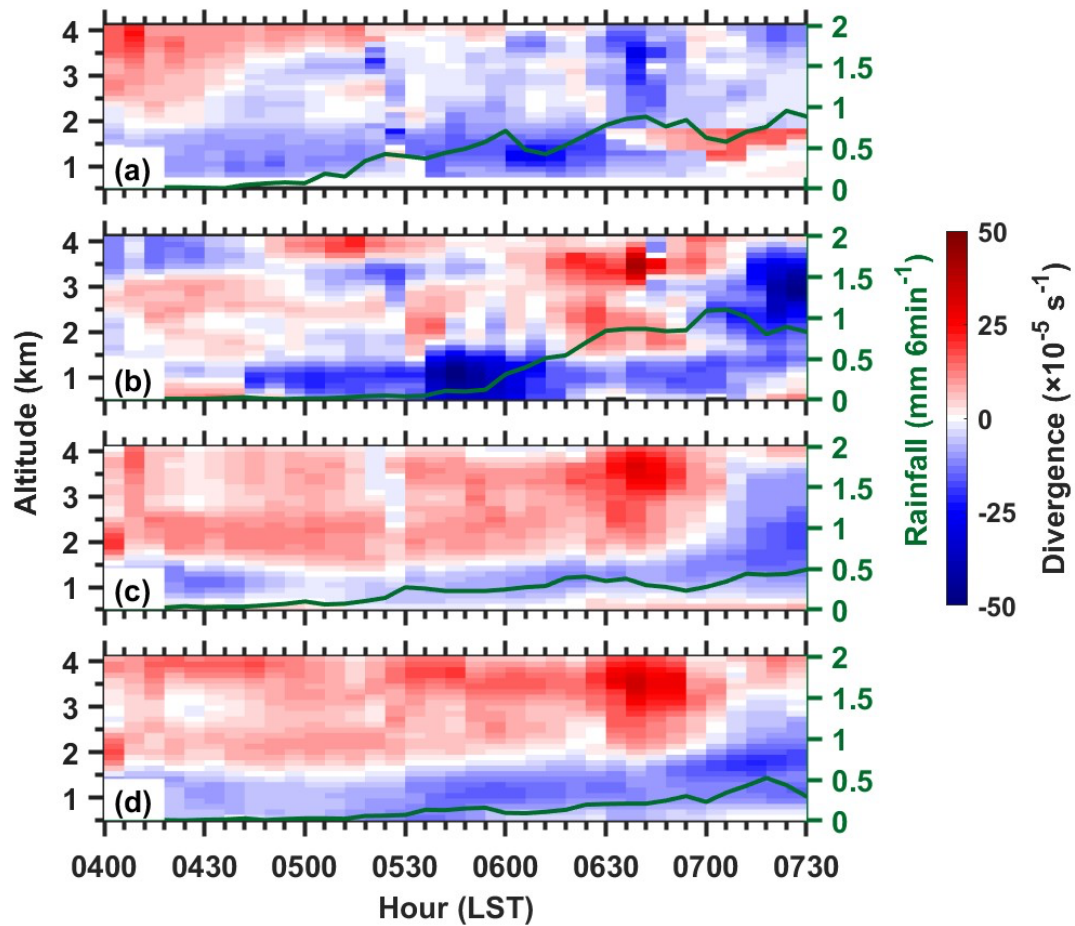


Figure 7. The vertical profiles of the triangle-averaged divergence (10^{-5} s^{-1} , shading) derived from the RWP mesonet in Beijing at 120 m vertical resolution between 0.51 and 4.11 km AMSL at 6-min intervals during the period of 0400–0730 LST 22 July, 2023 for (a) triangle 1, (b) triangle 2, (c) triangle 3, and (d) triangle 4 (see their distributions in Figure 1a). Green-dotted lines represent the triangle-area-averaged rainfall amount ($\text{mm } 6\text{min}^{-1}$).

As shown in Figure 7c and 7d, the relationship between vertical profiles of divergence and rainfall for triangle 3 and 4 during the rainy period was analogous to that for triangle 1 and 2. Nevertheless, triangle 3 and 4 experienced relatively weaker low-level convergence below 1.5 km AMSL. The presence of dominated divergence layer above is not conducive to the extension of upward movement and formation of convective clouds. The weaker peak area-averaged rainfall rate was seen in triangle 3 and 4 in contrast. Clearly, it has been proved that the RWP mesonet has the capability of detecting the continuous vertical profiles of divergence leading to the onset of precipitation at high spatial and temporal resolutions. However, the development of convection is also affected by many other thermal and dynamic variables, it should be noted that it's feasible to qualitatively determine the change of rainfall rather than quantitatively. ”